Postprint of: Szociński M., Darowicki K., Impedance evaluation of coatings from biobased material. Surface Innovations, 2018, Vol. 6, nr 4-5, pp. 286-294, DOI: 10.1680/jsuin.18.00016

Impedance evaluation of coatings from biobased material

Michał Szociński*, Ph.D., Assistant professor at Gdańsk University of Technology, Chemical Faculty, Department of Electrochemistry, Corrosion and Materials Engineering, 11/12 G. Narutowicza Str., 80-233, Gdańsk, Poland, michal.szocinski@pg.edu.pl, tel. +48583471273, fax +48583471092

Kazimierz Darowicki, Professor, Head of the department, Gdańsk University of Technology, Chemical Faculty, Department of Electrochemistry, Corrosion and Materials Engineering, 11/12 G. Narutowicza Str., 80-233, Gdańsk, Poland

*corresponding author

The authors proposed a modification of sodium caseinate edible coating for foodstuff protection. The aim was to improve the film's barrier properties. It was achieved by addition of propolis, which is a natural, environmentally friendly product, known from its intrinsic sealing action. In the next step, the propolis-admixed sodium caseinate films were exposed to elevated temperature for 10 minutes. This approach was meant to improve the barrier effect of propolis. Electrochemical impedance spectroscopy was used to evaluate performance of the control and modified samples upon immersion in water. The atomic force microscopy-based measurements visualized the sealing effect of propolis by means of topographical images, local dc current maps and local impedance spectra of the control and modified films. Obtained results allowed drawing a conclusion that the proposed modifications improved the barrier properties of the sodium caseinate films.

RESEARCH PAPER

GREEN COATINGS, CURRENT VOLTAGE CHARACTERISTICS, ATOMIC FORCE MICROSCOPY

Introduction

Increasing emphasis on environmental friendliness, ecology and green chemistry is also reflected in the field of organic protective coatings. These aspects are especially crucial in case of the coatings for foodstuff protection. A purpose of these coatings is to provide a semipermeable barrier between food and oxygen, moisture, solute movement as well as microbes of external source, in order to extend the shelf life of foodstuff.[1] Such coatings must not create any health hazard to potential consumers. Therefore, they have to be edible or easy to remove if they play the role of packaging materials.[2,3] Maintenance of aesthetic appearance is another function of the food coatings. They have to be transparent and they should even provide gloss to the foodstuff, such as fruit or vegetables.[4] The researchers also draw attention to different modifications of the edible films and their antimicrobial function.[5-7] Aforementioned specific demands, often contradictory in character, hinder identification of the optimal material fulfilling all the requirements. The edible coatings cover three main groups: hydrocolloids including polysaccharides and proteins, lipids including fatty acids and waxes as well as their composites.[8]

Skurtys and co-workers wrote a comprehensive contribution about the food hydrocolloid edible films and coatings.[9] Fabra et al. investigated the microstructure and optical properties of the sodium caseinate films containing oleic acid-beeswax mixtures.[10] They established a correlation between gloss, transparency and surface roughness of the films. Shou and co-workers examined influence of glycerol-protein ratio on the maximum load, tensile strength, elastic modulus and moisture content of the sodium caseinate films.[11] Such parameters as uniform and controlled film thickness, less cross-contamination and simplicity of its application in a production scale should be taken into account upon evaluation of food coatings functionality. Andrade et al. discussed those aspects with respect to the atomizing spray systems for edible coatings.[12] Park pointed out the problems and challenges associated with the food coatings.[13] He put an emphasis on gas permeation and diffusivity through the edible coatings. In their review paper, Lin and Zhao presented the analytical techniques employed for measuring the performance of the edible coatings applied on fruit and vegetables.[14] They highlighted such aspects as internal gas composition of coated product, coating thickness, wettability and surface characteristics of the coatings. Albert and Mittal compared several edible coatings regarding their film forming ability, water and fat transfer properties as well as suitability for fried food.[15] Jaramillo et al. revealed the plasticization and improved biodegradability effects of the yerba mate extract in starch edible films.[16] Thakur and others focused on optimization of the pea starch–chitosan edible film formulation by implementing the response surface methodology.[17] Some

edible coatings take the form of bionanocomposite, for instance the whey protein isolate based films embedded with zein nanoparticles, which were investigated by Oymaci and Altinkaya.[18]

The aim of this paper is to present improvement in barrier properties of the edible sodium caseinate coating due to a proposed modification. The modification consists in admixing of sodium caseinate with propolis and optional, post-application heating of the newly established coating. Propolis was selected as a natural, environmentally friendly product, which complies with the health restrictions for edible coatings. In nature, propolis, also called a 'bee glue', is used as a sealant for unwanted open spaces in honey bees hive. This property is employed in our investigations. The post-application exposure to elevated temperature provides additional sealing of the pores in the propolis-admixed sodium caseinate coating. Electrochemical impedance spectroscopy (EIS) and atomic force microscopy (AFM) techniques were used to evaluate the tested coatings.

Experimental

The investigation was performed for three groups of samples:

(i) pure sodium caseinate coating (control sample),
(ii) sodium caseinate coating admixed with propolis,
(iii) sodium caseinate coating admixed with propolis and post-application heated.

All the coatings were applied on the steel substrates using the Elcometer 3540 bar coater. The substrates were prepared by grinding and polishing with the following abrasive paper grades: P800 (average particle size 21.8μm), P1500 (average particle size 12.6μm), P2500 (average particle size 8.4μm), P3000 (average particle size 6.0μm) and P4000 (average particle size 2.5μm). Then they were degreased with acetone. After coating application, the samples were dried for 24h at 45%RH in 20°C. The Surfix E-FN gauge by Phynix Co. was used for coating thickness measurement. The measurements were carried out at 20 spots on the surface of each sample and then mean value was calculated. The films thickness amounted 20 ± 2μm for the pure sodium caseinate coating and 21± 2μm for the propolis-admixed coating. The pure sodium caseinate film was prepared from 8% (w/w) aqueous solution containing glycerol as a plasticizer. The protein : plasticizer ratio was 1 : 0.3 (w/w). The mixture was homogenized for 5 minutes at 20 000 r.p.m. Sodium caseinate, which was a film-forming component, was obtained from the Acros Organics, Geel, Belgium. The propolis-admixed sodium caseinate coating was prepared in an analogous way to the pure sodium caseinate film. Additionally, propolis was added in the protein : lipid ratio equal 1 : 0.08 (w/w). Propolis was provided as 7% ethanol solution (Farmapia, Cracow, Poland). The third group of samples consisted of the propolis-admixed sodium caseinate film, which after application and drying were additionally exposed to the elevated temperature of 50°C for 10 minutes. This operation was aimed at plasticization of propolis, which was expected to seal potential pores and defects present in the film. Five samples of each system were investigated. The paper presents exemplary results, representative for behaviour of each group of the samples.

State and durability of the investigated coatings were evaluated and compared upon water immersion. Electrochemical impedance spectroscopy was used for this purpose. Moreover, atomic force microscopy was utilized to characterize initial condition of the investigated coatings.

Electrochemical impedance spectroscopy measurements

The EIS measurements were carried out in a two-electrode system. The coated steel substrate was a working electrode and a platinum mesh served as a counter electrode. The measurements were executed upon immersion in water. Investigated surface area of the sample equalled 5.3cm^2. An experimental set-up consisted of the Schlumberger 1255 frequency response analyser coupled to the high input impedance buffer Atlas 9181. Impedance spectra were recorded in the frequency range from 1MHz to 10mHz. Ten points were measured per each frequency decade. The perturbation signal amplitude was 10mV.

Atomic force microscopy measurements

The AFM-based technique, utilized in our studies, was originally proposed by Kalinin et al. for investigation of polycrystalline ZnO.[19] However, we adopted it to a research in the field of coatings and thin protective layers.[20-25] The technique was also utilized by O'Hayre et al. to study solid polymer electrolytes, polycrystalline ZnO varistors and microscale test patterns of different electrical characteristics.[26,27] This contact mode, AFM-based approach allows local impedance imaging[28] and spectroscopy.[29] Details of the technique have been described by the authors elsewhere.[30] One of the advantages of this AFM-based approach is a possibility to conduct the measurements in dry conditions, with no need for electrolyte presence. Most of the local techniques for coatings and thin films investigation are electrochemical in character, so they require electrolytic conditions. Wittmann et al. used a five-electrode system with a split microreference electrode to detect local coating heterogeneities.[31] Local impedance mapping was employed to identify undercoating corrosion of aluminium alloy upon exposure to chloride solution.[32,33] Jorcin and co-workers utilized local electrochemical impedance approach to follow delamination progress beneath organic coating.[34] Numerous investigations take advantage of the method reported by Lillard et al., which

employs two-microelectrodes to measure local ac solution current density above the investigated surface to determine local impedance.[35] Zou and Thierry utilized this approach to measure blistering of the coating.[36]

An atomic force microscope employed in the studies was the SPM Ntegra Aura system by the NT-MDT Co.. The measurements were performed in dry conditions, without immersion in electrolyte. The maximum scan area equalled 8100μm^2 (90μmx90μm). The AFM probe was diamond coated. The measurements were executed in a contact, scanning by the tip mode. The scanning frequency was 0.8Hz. The Nova software by the NT-MDT Co. was used for recording, processing and analysis of the images. Local dc current maps were acquired for the bias voltage of 20mV applied between the AFM tip and the coated substrate.

Local impedance spectra were collected in a stationary regime with the AFM tip placed at the spot of interest. A measurement set-up consisted of the Parstat 2236 workstation configured in a two-terminal measurement mode. One terminal was connected to the coated steel substrate, the second one was in contact with a conductive layer of the AFM probe. The local impedance spectra were recorded in the frequency range from 0.1MHz to 1Hz. Thirty points were measured per each frequency decade. The amplitude of perturbation voltage was 100mV.

Results and discussion

After coating drying, the samples were immersed in water for 24h and the impedance spectra were collected at 1-hour intervals. This time span turned out sufficient to demonstrate effectiveness of proposed coating modification. Long-term performance of the coatings was not the subject of investigation. Fig. 1 presents the exemplary spectra, in the Nyquist format, collected for the pure sodium caseinate film. In each case, there are two time constants visible in the spectrum. The high-frequency semicircle diameter, corresponding to film properties, is of a few hundred ohms order. It is an evidence that pure sodium caseinate does not constitute a tight barrier for water ingress. Appearance of the low-frequency time constant confirms this observation and indicates electrochemical reaction at the coating/substrate interface. The shape of spectra and the magnitude of impedance do not change significantly with time of exposure to water. The investigated system attains stability within first few hours of immersion.

Figure 1.

Fig. 2 shows the exemplary impedance spectra, in the Nyquist format, recorded for the propolis-admixed sodium caseinate film. They also exhibit at least two time constants. However, the high frequency semicircles, corresponding to coating properties, indicate higher impedance than for the pure sodium caseinate layer. The difference is about one order of magnitude.

Figure 2.

Fig. 3 depicts one of the electrical equivalent circuits, which can be used to describe non-barrier, defected coating. Coating pore resistance (R_c) and coating capacitance (C_c), in this case represented by a constant phase element, refer to condition of the film. Hence, these parameters were of our interest as the aim was to analyse the coating properties only. Remaining two parameters of the circuit – charge transfer resistance (R_{ct}) and electrical double layer capacitance (C_{dl}) – are related to corrosion reaction at the coating/substrate interface. They can be evaluated using low-frequency region of the impedance spectrum. However, this part of the spectrum was interpreted only qualitatively to acknowledge electrochemical activity at the interface. Our intention was not to describe these processes in quantitative manner.

Figure 3.

Fig. 4 illustrates evolution of the coating pore resistance during the 24-hour immersion in water. It compares behaviour of the pure sodium caseinate and propolis-admixed sodium caseinate films as well as the propolis-admixed sodium caseinate coating, which was additionally exposed to elevated temperature prior to the investigation. Incorporation of propolis contributes to significant, as for that type of the coating, increase in resistance of the sodium caseinate film. The propolis-admixed film exhibits about one order of magnitude higher resistance than the pure sodium caseinate coating. Moreover, a short exposure to elevated temperature brings further benefit to barrier properties of the propolis-admixed coating. High temperature leads to propolis plasticization and makes it seal some of the pores in the sodium caseinate coating. This is manifested by an increase in the coating pore resistance from ca. 1.5kΩcm^2 (the propolis-admixed film) to ca. 3.5kΩcm^2 (the admixed and heated film). It is also evident that the coating pore resistance of each sample is stable versus time. There are some oscillations around fixed values, however even for the most unstable course (the admixed and heated coating) they do not exceed the amplitude of 0.5kΩcm^2.

Figure 4.

The changes of the *Q* parameter of constant phase element (CPE), corresponding to capacitive behaviour of coating, reveal characteristic trends, too (Fig. 5). The pure sodium caseinate film has the highest capacitance of ca. 400μF/cm^2, which remains at similar level for most of the 24-hour exposure. Addition of propolis results in a decrease in capacitance by about 100μF/cm^2. Optionally heated, propolis-admixed coating exhibits slightly lower capacitance during the first half of the test (up to ca. 12th hour of immersion). Then the capacitance values of the heated and non-heated propolis-admixed samples are comparable. There can be at least two explanations of observed trends in capacitance evolution. The decrease in coating capacitance after addition of propolis could be caused by lower water absorption due to addition of hydrophobic, water insoluble propolis. Simultaneously, a decrease in effective area of the coating occurred due to lower amount of pores in the film, which contributed to a decrease in the coating capacitance. Sealing of the coating with propolis is illustrated and discussed in the following part of this chapter concerning the AFM measurements. Similar explanations can be addressed to behaviour of the heated, propolis-admixed film. Further decrease in the number and size of pores contributed to lower surface area of the coating. Slightly lower capacitance revealed during the first twelve hours of immersion is probably due to higher initial coating resistance to water uptake.

Figure 5.

The pure sodium caseinate coating exhibits the highest value of the *n* parameter of CPE, oscillating around 0.75 for most of the exposure time (Fig. 6). It can be explained by uniformity of film composition because in majority it consists of one compound – sodium caseinate. Nevertheless, there is a deviation from ideal behaviour due to presence of multiple pores in the film. Introduction of propolis results in a decrease in composition homogeneity of the film, which is reflected in lower magnitude of the *n* parameter (it amounts 0.63). The interpretation of this effect is troublesome. On one hand one could expect improvement of coating uniformity due to sealing effect of propolis. However, it seems that phenomenon was offset, at least to some extent, by introduction of foreign material (propolis) to the sodium caseinate matrix. Heating provides the coating with slightly higher uniformity (*n* parameter of ca. 0.68) as compared to the non-heated, propolis-admixed sodium caseinate film. As at that stage no additional component was introduced into the coating matrix, this improved uniformity can be attributed exclusively to further decrease in the number and size of pores due to more even propolis dispersion. For each sample, the course of the *n* parameter versus time of exposure is stable, without any sharp deviations from an average level.

Figure 6.

The atomic force microscopy measurements were carried out prior to water immersion of the samples. The aim was visualization of differences in topography of the synthesized coating types (Figs 7a-c). Each investigated film exhibits different porosity. The most porous is the pure sodium caseinate coating (Fig. 7a), with a lot of cavities all over the AFM image. Admixing with propolis results in the surface with less pores, although still they are distributed over the entire AFM image (Fig. 7b). Clear improvement in the coating quality occurs for the propolis-admixed film exposed to elevated temperature. Fig. 7c depicts the surface with the smallest number of pores, which also have significantly smaller diameter.

Figure 7a.

Figure 7b.

Figure 7c.

Recorded AFM topographical images were subjected to a surface roughness analysis. Table 1 presents the results of this analysis in terms of the ten point height parameter (S_{10z}). The pure sodium caseinate film is characterized by the highest surface roughness equal 1.72μm. Addition of propolis resulted in a decrease in surface roughness by 0.23μm. It may not be a substantial decrement, nevertheless, it confirms the observations stemming from a comparison of Fig. 7a and Fig. 7b. Admixing with propolis decreased the number of pores in the film, which was reflected in slightly lower surface roughness. The biggest effect is exhibited by the propolis-admixed and heated film. In this case the S_{10z} parameter is more than two and a half times lower than for the pure sodium caseinate coating. This is a significant decrease, which confirms beneficial influence of the heating process. The lowest surface roughness also correlates with the topographical AFM image in Fig. 7c. Clearly lower number of pores and their smaller diameter are reflected in the lowest value of the S_{10z} parameter determined.

Table 1.

A relation between coating porosity and its barrier performance was established by measurement of local dc current maps using the atomic force microscope (Figs 8a-c). Bright spots indicate the regions where the coating does not constitute a barrier for direct current flow. These areas are conductive and do not provide protection of the metal substrate. The pure sodium caseinate film exhibits the largest fraction of unprotected area (Fig. 8a). The sealing effect, due to propolis application, is evident in Fig. 8b and Fig. 8c, which represent the dc current maps of the propolis-admixed and optionally heated coatings, respectively. These two coating types reveal decreasing fraction of surface occupied by conductive regions. It is an evidence of barrier properties improvement thanks to the proposed modification.

Figure 8a.

Figure 8b.

Figure 8c.

The local impedance spectra, recorded with the AFM-based approach, are another evidence of differentiated electrical and protective properties of the investigated coatings, depending on localization on the specimens surface.

Figure 9.

Figure 9 shows an exemplary topographical image of the propolis-admixed sodium caseinate coating with the indications of the spots where the local impedance spectra were collected. The impedance in the spectrum collected inside a pore of the coating (Fig. 10) is ca. three orders of magnitude lower than the impedance in the spectrum recorded on an intact coating region (Fig. 11). The impedance measured on bare steel substrate inside the pore is of megaohms order, while the impedance on intact film reaches gigaohms order. Both values seem quite high, especially as compared to the global impedance measurement. The latter provides the information averaged over the entire surface under investigation (5.3cm^2). In this case both intact and porous regions of the coating contribute to the magnitude of global impedance, which amounts a few kiloohms. Moreover, the measurements were carried out in electrolyte. The local impedance spectra were collected in dry conditions, without electrolyte. Local impedance is a sum of AFM tip impedance, tip-sample contact impedance and investigated material impedance. These facts explain higher impedance on local impedance spectra. Nevertheless, relative differences in local impedance make it possible to spatially resolve the places covered with the protective film from those where bare substrate is exposed. Local impedance spectra are another approach, which allows evaluation of an extent and surface distribution of the protective effect due to the proposed modification of the sodium caseinate coating.

Figure 10.

Figure 11.

Summarizing, the results of electrochemical impedance spectroscopy and atomic force microscopy investigations are consistent and complementary. They show that the proposed modification of the sodium caseinate coating with propolis contributes to improvement of the film's barrier character. The properties of propolis and the optional heating procedure provide a sealing effect as compared to the pure sodium caseinate film. It is manifested by an increase in the film impedance, decreased coating porosity and surface roughness as well as decreased local dc current conductivity over the investigated surface area.

Conclusion

Performed research allows stating the following conclusions:

- admixing of the sodium caseinate food coating with propolis resulted in an increase in film impedance by about one order of magnitude when measured upon water immersion service,
- additional, pre-service exposure of the propolis-admixed coating to elevated temperature yielded further increase in film impedance,
- addition of propolis contributed to a decrease in the number of pores in the sodium caseinate coating, which was proved with the atomic force microscopy measurements,

- pre-service heating of the propolis-admixed coating provided further decrease in the number and size of film pores, which was confirmed by the AFM topographical image,
- analysis of the AFM topographical images revealed a decrease in surface roughness of the sodium caseinate coating due to propolis admixing and pre-service heating – from S_{10z}=1.72μm for the pure sodium caseinate film to S_{10z} =0.65μm for the propolis-modified and heated coating,
- local dc current maps, obtained with the AFM approach, revealed a decrease in the number of through-the-coating defects when the sodium caseinate film was admixed with propolis; further decrease in the surface fraction occupied by conductive regions was noticed for the propolis-admixed and heated coating,
- proposed modification of the sodium caseinate film, consisting in addition of propolis and optional heating, was successful and resulted in improvement of barrier properties of the coating,
- atomic force microscopy topographical images, local dc current maps and local impedance spectra illustrated the sealing effect due to admixed propolis, which accounted for improvement of barrier properties,
- applied combination of the investigation methods, electrochemical impedance spectroscopy and atomic force microscopy, allowed successful characterization of protective properties of sodium caseinate coatings,
- proposed atomic force microscopy measurement modes can be employed for evaluation of modifications implemented into biobased coatings, especially when there is a need for electrolyteless tests,
- investigated coating and our modifications are natural, ecological and environmentally friendly; these are not only indispensable features of edible food coatings, but they also follow increasingly emphasized "green chemistry" attitude,
- biobased, green coatings constitute interesting candidates for temporary anticorrosion protection, for instance during transport and storage, which is an incentive for further studies.

References

1. Dhall RK (2013) Advances in edible coatings for fresh fruits and vegetables: a review. *Critical Reviews in Food Science and Nutrition* **53**: 435-450.
2. Tambe C, Graiver D and Narayan R (2016) Moisture resistance coating of packaging paper from biobased silylated soybean oil. *Progress in Organic Coatings* **101**: 270–278.
3. Khwaldia K, Arab-Tehrany E and Desobry S (2010) Biopolymer coatings on paper packaging materials. *Comprehensive Reviews in Food Science and Food Safety* **9**: 82-91.
4. Trezza TA and Krochta JM (2000) The gloss of edible coatings as affected by surfactants, lipids, relative humidity and time. *Journal of Food Science* **65(4)**: 658-662.
5. Campos CA, Gerschenson LN and Flores SK (2011) Development of edible films and coatings with antimicrobial activity. *Food and Bioprocess Technology* **4**: 849–875.
6. Ochoa TA, García Almendárez BE, Reyes AA, Rivera Pastrana DM, Gutiérrez López GF, Belloso OM and Regalado- González C (2017) Design and characterization of corn starch edible films including beeswax and natural antimicrobials. *Food and Bioprocess Technology* **10**: 103–114.
7. Kristo E, Koutsoumanis KP and Biliaderis CG (2008) Thermal, mechanical and water vapour barrier properties of sodium caseinate films containing antimicrobials and their inhibitory action on Listeria monocytogenes. *Food Hydrocolloids* **22**: 373–386.
8. Raghav PK, Agarwal N and Saini M (2016) Edible coating of fruits and vegetables: a review. *International Journal of Scientific Research and Modern Education (IJSRME)* ISSN (online) **2455-5630**: 188-204.
9. Skurtys O, Acevedo C, Pedreschi F, Enrione J, Osorio F and Aguilera JM (2010) Food hydrocolloid edible films and coatings. *In Food Hydrocolloids: Characteristics, Properties and Structures*. Nova Science Publishers Inc., pp. 41-80.
10. Fabra MJ, Talens P and Chiralt A (2009) Microstructure and optical properties of sodium caseinate films containing oleic acid–beeswax mixtures. *Food Hydrocolloids* **23**: 676-683.
11. Schou M, Longares A, Montesinos-Herrero C, Monahan FJ, O'Riordan D and O'Sullivan M (2005) Properties of edible sodium caseinate films and their application as food wrapping. *LWT* **38**: 605–610.
12. Andrade RD, Skurtys O and Osorio FA (2012) Atomizing spray systems for application of edible coatings. *Comprehensive Reviews in Food Science and Food Safety* **11**: 323-337.
13. Park HJ (1999) Development of advanced edible coatings for fruits. *Trends in Food Science and Technology* **10**: 254-260.
14. Lin D and Zhao Y (2007) Innovations in the development and application of edible coatings for fresh and minimally processed fruits and vegetables. *Comprehensive Reviews in Food Science and Food Safety* **6**: 60-75.

15. Albert S and Mittal GS (2002) Comparative evaluation of edible coatings to reduce fat uptake in a deep-fried cereal product. *Food Research International* **35**: 445–458.
16. Jaramillo CM, Gutiérrez TJ, Goyanes S, Bernal C and Fama L (2016) Biodegradability and plasticizing effect of yerba mate extract on cassava starch edible films. *Carbohydrate Polymers* **151**: 150–159.
17. Thakur R, Saberi B, Pristijono P, Stathopoulos CE, Golding JB, Scarlett CJ, Bowyer M and Vuong QV (2017) Use of response surface methodology (RSM) to optimize pea starch–chitosan novel edible film formulation. *Journal of Food Science and Technology* **54(8)**: 2270–2278.
18. Oymaci P and Altinkaya SA (2016) Improvement of barrier and mechanical properties of whey protein isolate based food packaging films by incorporation of zein nanoparticles as a novel bionanocomposite. *Food Hydrocolloids* **54**: 1-9.
19. Shao R, Kalinin SV and Bonnell DA (2003) Local impedance imaging and spectroscopy of polycrystalline ZnO using contact atomic force microscopy. *Applied Physics Letters* **82:** 1869-1871.
20. Szociński M, Darowicki K and Schaefer K (2010) Identification and localization of organic coating degradation onset by impedance imaging. *Polymer Degradation and Stability* **95(6)**: 960-964.
21. Szociński M and Darowicki K (2014) Local properties of organic coatings close to glass transition temperature. *Progress in Organic Coatings* **77(12)**: 2007-2011.
22. Darowicki K and Szociński M (2007) Local impedance spectroscopy of membranes. *Journal of Membrane Science* **303(1-2)**: 1-5.
23. Szociński M (2016) Evaluation of organic coatings condition with AFM-based method. *Surface Innovations* **4(2)**: 70-75.
24. Szociński M and Darowicki K (2016) Performance of zinc-rich coatings evaluated using AFM-based electrical properties imaging. *Progress in Organic Coatings* **96**: 58-64.
25. Szociński M (2016) AFM-assisted investigation of conformal coatings in electronics. *Anti-Corrosion Methods and Materials* **63(4)**: 289-294.
26. O'Hayre R, Lee M and Prinz FB (2004) Ionic and electronic impedance imaging using atomic force microscopy. *Journal of Applied Physics* **95**: 8382-8392.
27. O'Hayre R, Feng G, Nix WD and Prinz FB (2004) Quantitative impedance measurement using atomic force microscopy. *Journal of Applied Physics* **96**: 3540-3549.
28. Szociński M, Darowicki K and Schaefer K (2013) Application of impedance imaging to evaluation of organic coating degradation at a local scale. *Journal of Coatings Technology and Research* **10(1)**: 65-72.
29. Szociński M and Darowicki K (2013) Local impedance spectra of organic coatings. *Polymer Degradation and Stability* **98(1)**: 261-265.
30. Darowicki K, Szociński M and Zieliński A (2010) Assessment of organic coating degradation via local impedance imaging. *Electrochimica Acta* **55(11)**: 3741-3748.
31. Wittmann MW, Leggat RB and Taylor SR (1999) The detection and mapping of defects in organic coatings using local electrochemical impedance methods. *Journal of the Electrochemical Society* **146***:* 4071–4075.
32. Mierisch AM, Yuan J, Kelly RG and Taylor SR (1999) Probing coating degradation on AA2024-T3 using local electrochemical and chemical techniques. *Journal of the Electrochemical Society* **146**: 4449–4454.
33. Mierisch AM, Taylor SR (2003) Understanding the degradation of organic coatings using local electrochemical impedance methods - I. Commonly observed features. *Journal of the Electrochemical Society* **150**: B303-B308.
34. Jorcin JB, Aragon E, Merlatti C and Pebere N (2006) Delaminated areas beneath organic coating: a local electrochemical impedance approach. *Corrosion Science* **48**: 1779–1790.
35. Lillard RS, Moran PJ and Isaacs HS (1992) A novel method for generating quantitative local electrochemical impedance spectroscopy. *Journal of the Electrochemical Society* **139**: 1007–1012.
36. Zou F and Thierry D (1997) Localized electrochemical impedance spectroscopy for studying the degradation of organic coatings. *Electrochimica Acta* **42:** 3293–3301.

Figure captions

Figure 1 *Exemplary impedance spectra of the pure sodium caseinate film on steel collected during 24-hour immersion in water.*

Figure 2 *Exemplary impedance spectra of the propolis-admixed sodium caseinate film on steel collected during 24-hour immersion in water.*

Figure 3 *Electrical equivalent circuit representing non-barrier coating with electrochemical reaction at the coating/metal substrate interface: R_s is the solution resistance, R_c denotes the coating pore resistance, C_c is the coating capacitance represented by CPE (Q, n), R_{ct} is the charge transfer resistance and C_{dl} corresponds to the electrical double layer capacitance.*

Figure 4 *Evolution of the coating pore resistance during 24-hour immersion in water.*

Figure 5 *Evolution of the Q parameter of CPE during 24-hour immersion in water.*

Figure 6 *Evolution of the n parameter of CPE during 24-hour immersion in water.*

Figure 7 *Exemplary AFM topographical images of the investigated coatings, collected prior to immersion exposure for: (a) the pure sodium caseinate film, (b) the propolis-admixed sodium caseinate film, (c) the propolis-admixed sodium caseinate film heated at 50° C for 10 minutes.*

Figure 8 *Exemplary local dc current maps of the investigated coatings, collected prior to the immersion exposure for: (a) the pure sodium caseinate film, (b) the propolis-admixed sodium caseinate film, (c) the propolis-admixed sodium caseinate film heated at 50° C for 10 minutes.*

Figure 9 *Exemplary AFM topographical image of the propolis-admixed sodium caseinate film with marked places of local impedance spectra collection (A, B).*

Figure 10 *A local impedance spectrum collected inside the pore of the propolis-admixed sodium caseinate coating (the spot A in Fig. 9).*

Figure 11 *A local impedance spectrum collected on the intact region of the propolis-admixed sodium caseinate coating (the spot B in Fig. 9).*

List of tables

Figure 1

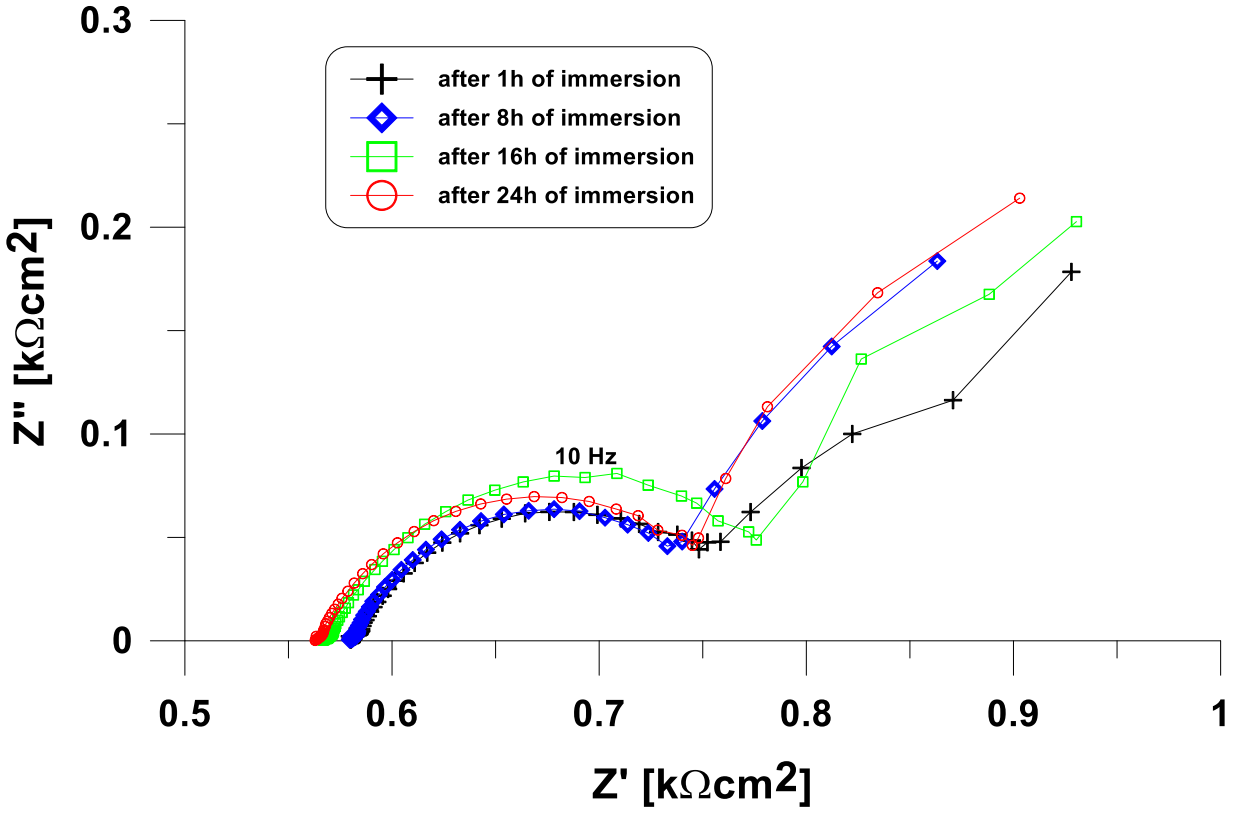

Figure 2

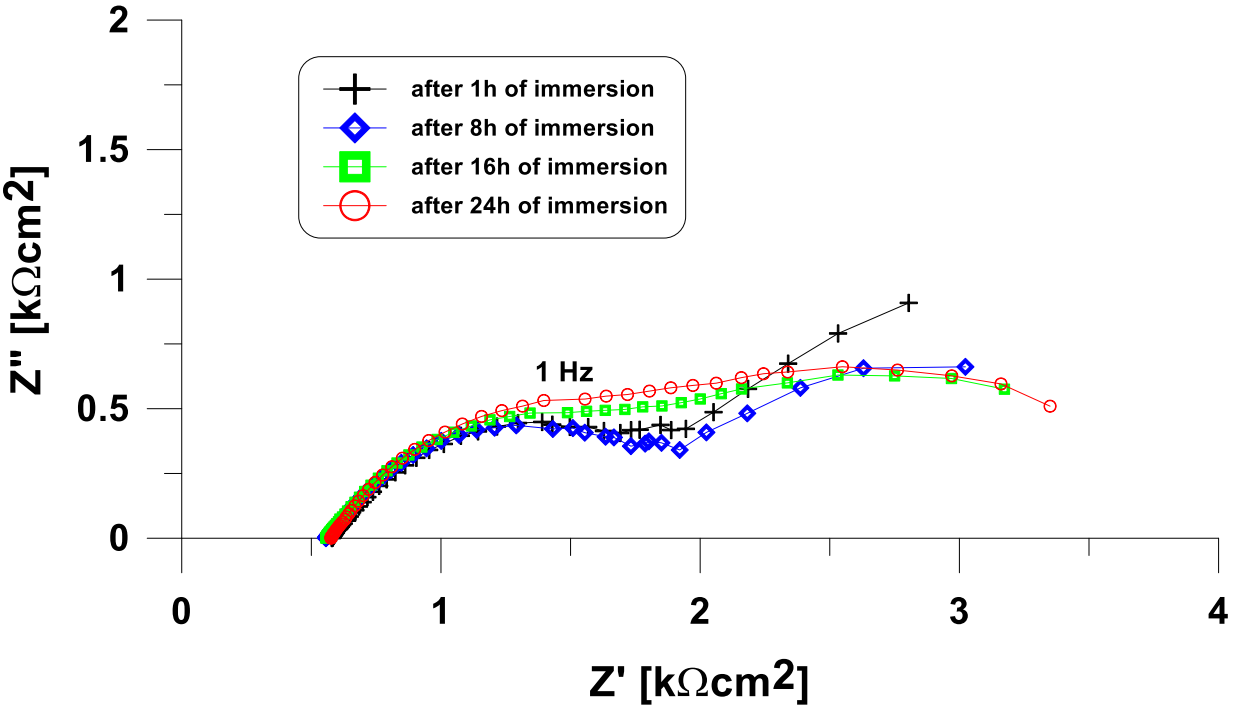

Figure 3

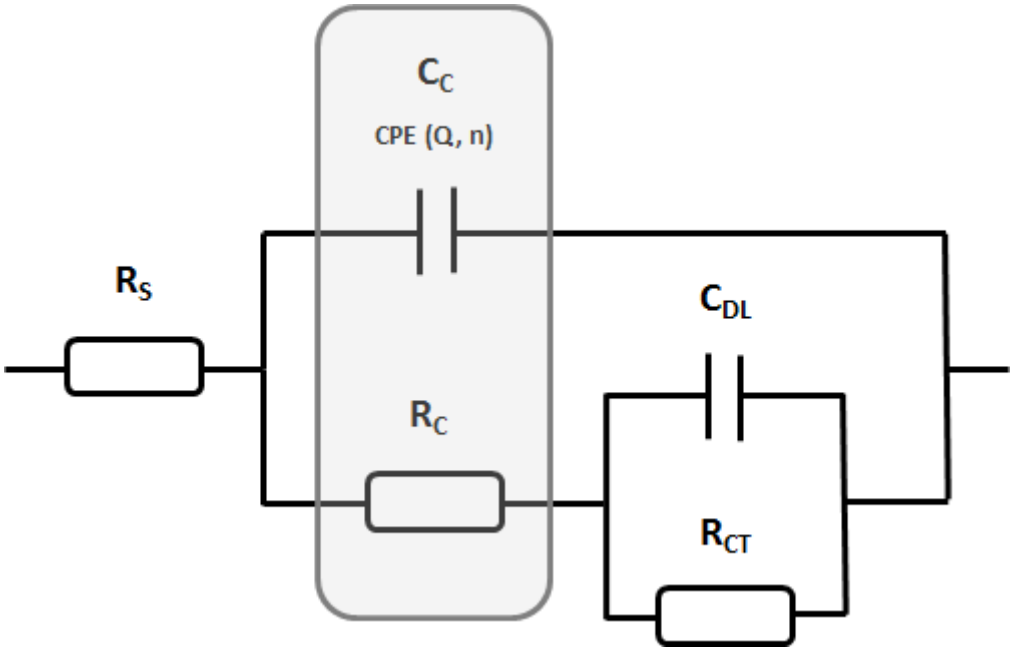

Figure 4

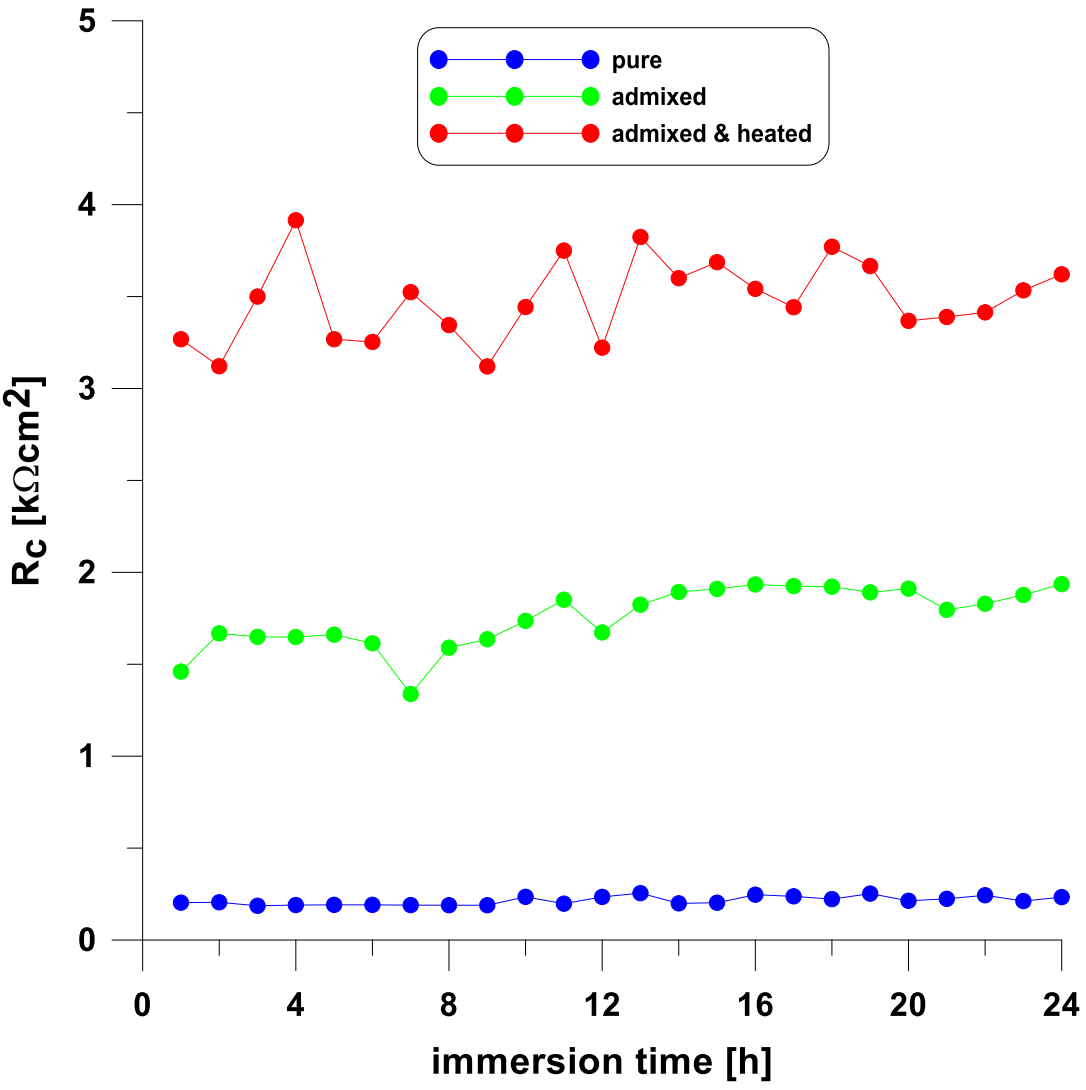

Figure 5

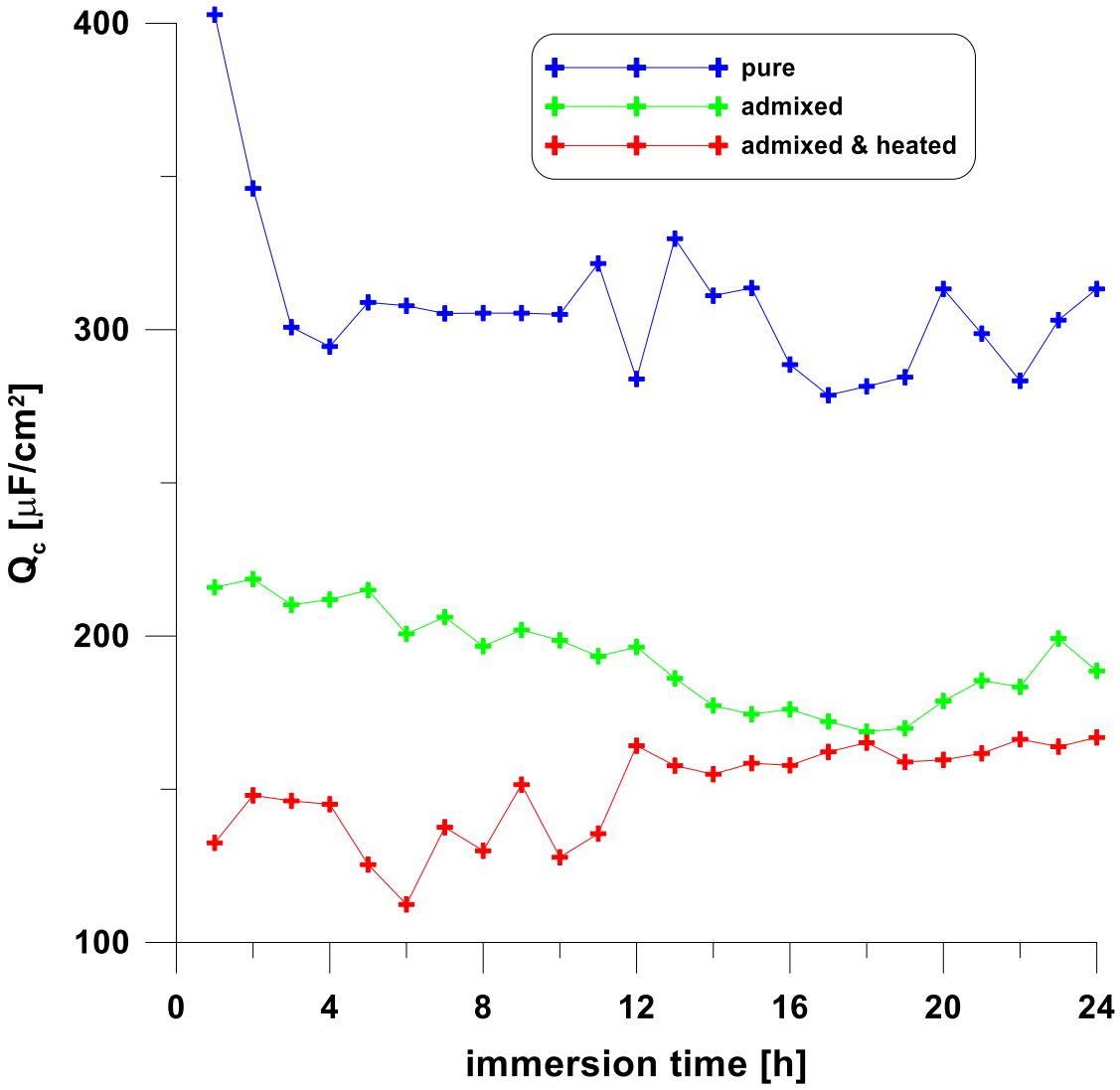

Figure 6

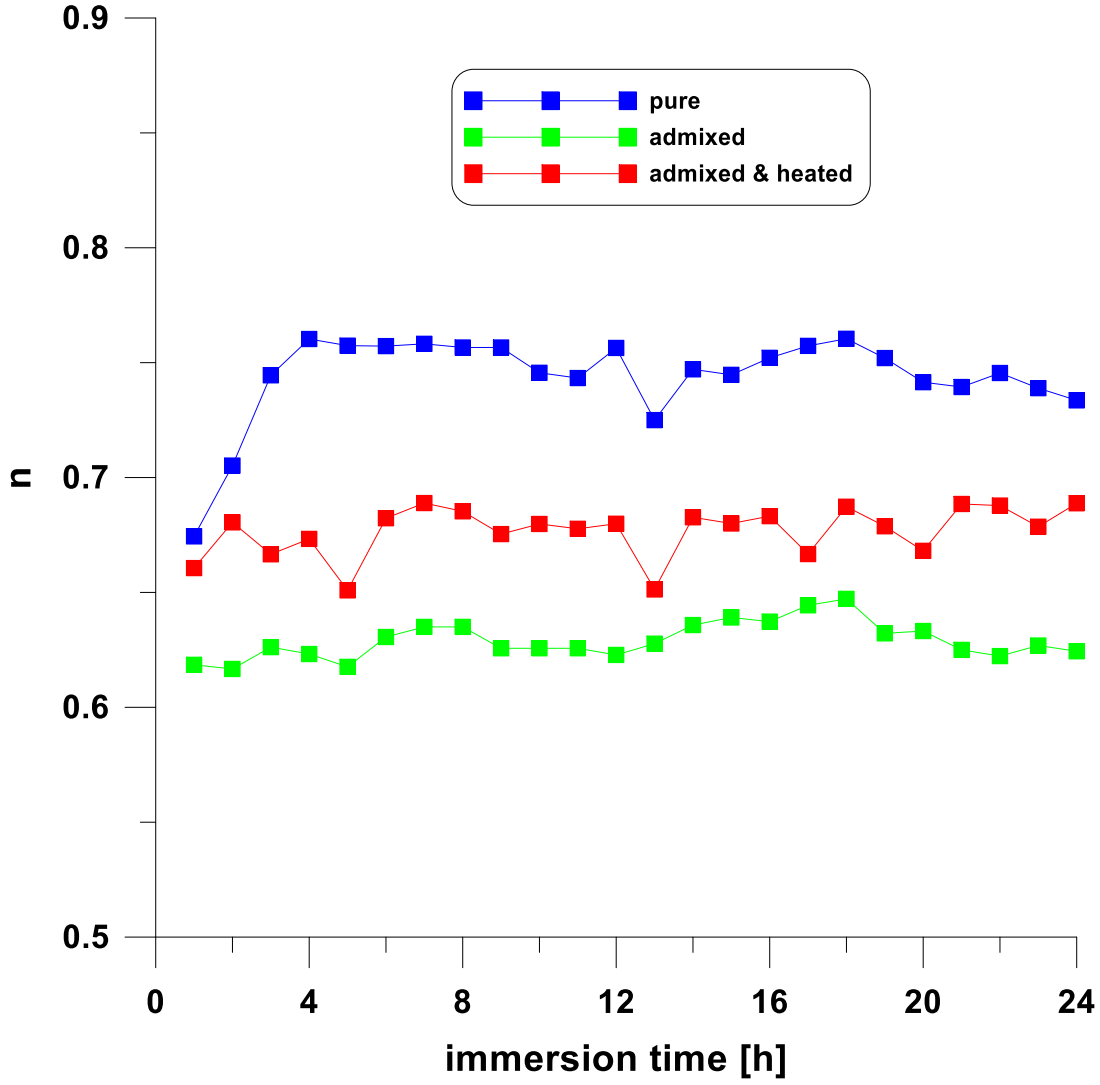

Figure 7a

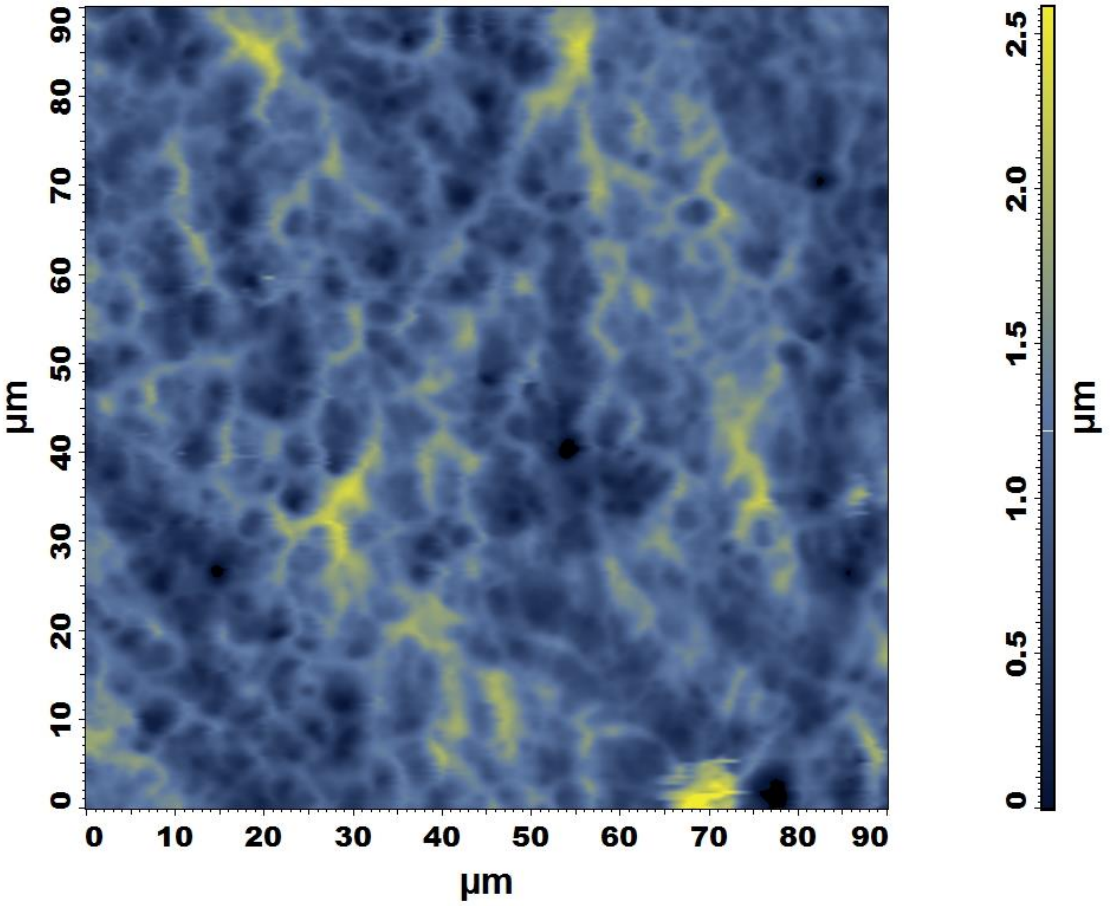

Figure 7b

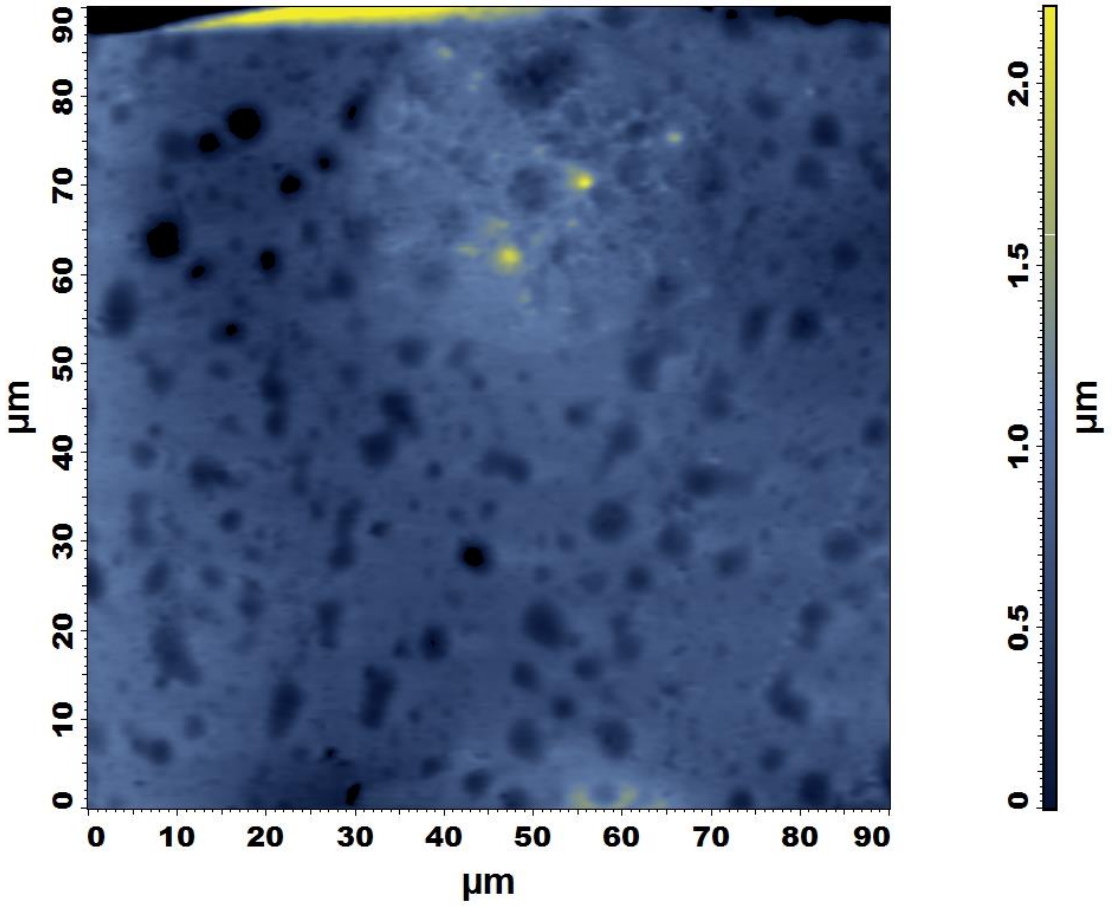

Figure 7c

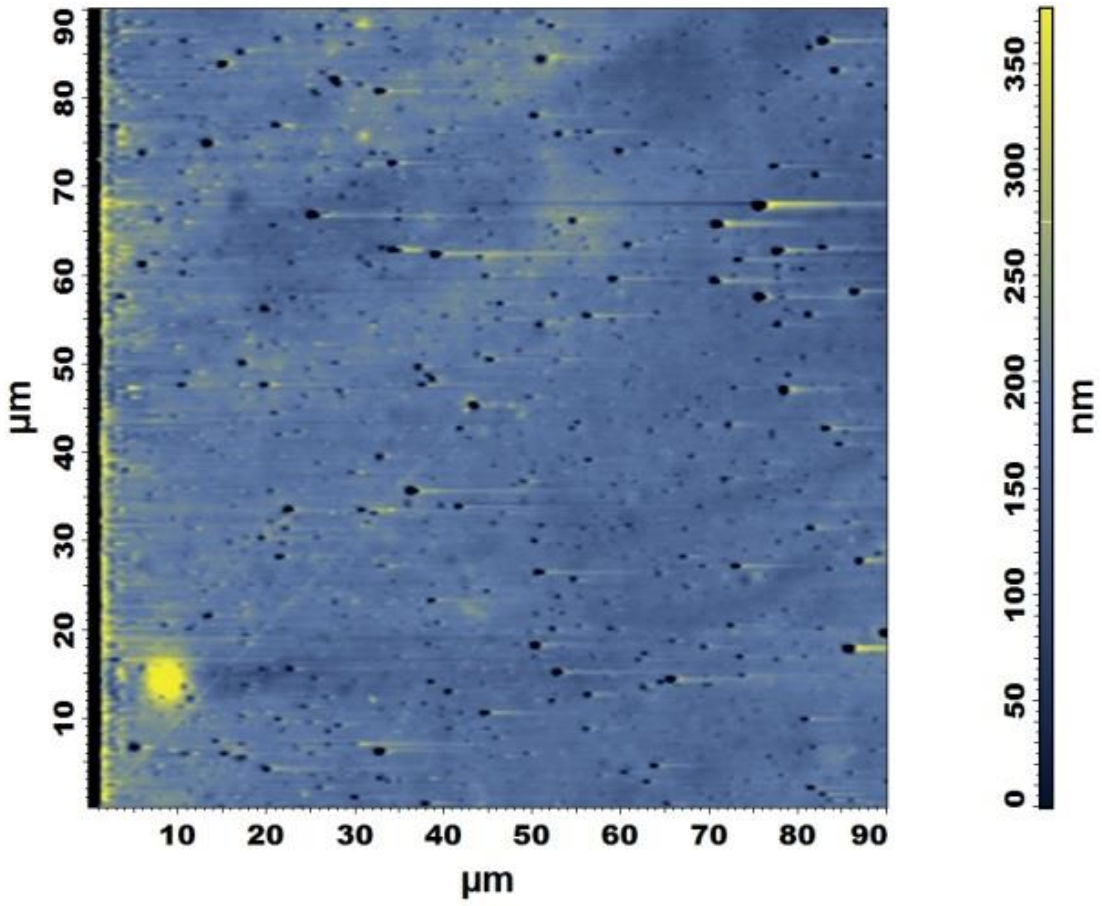

Figure 8a

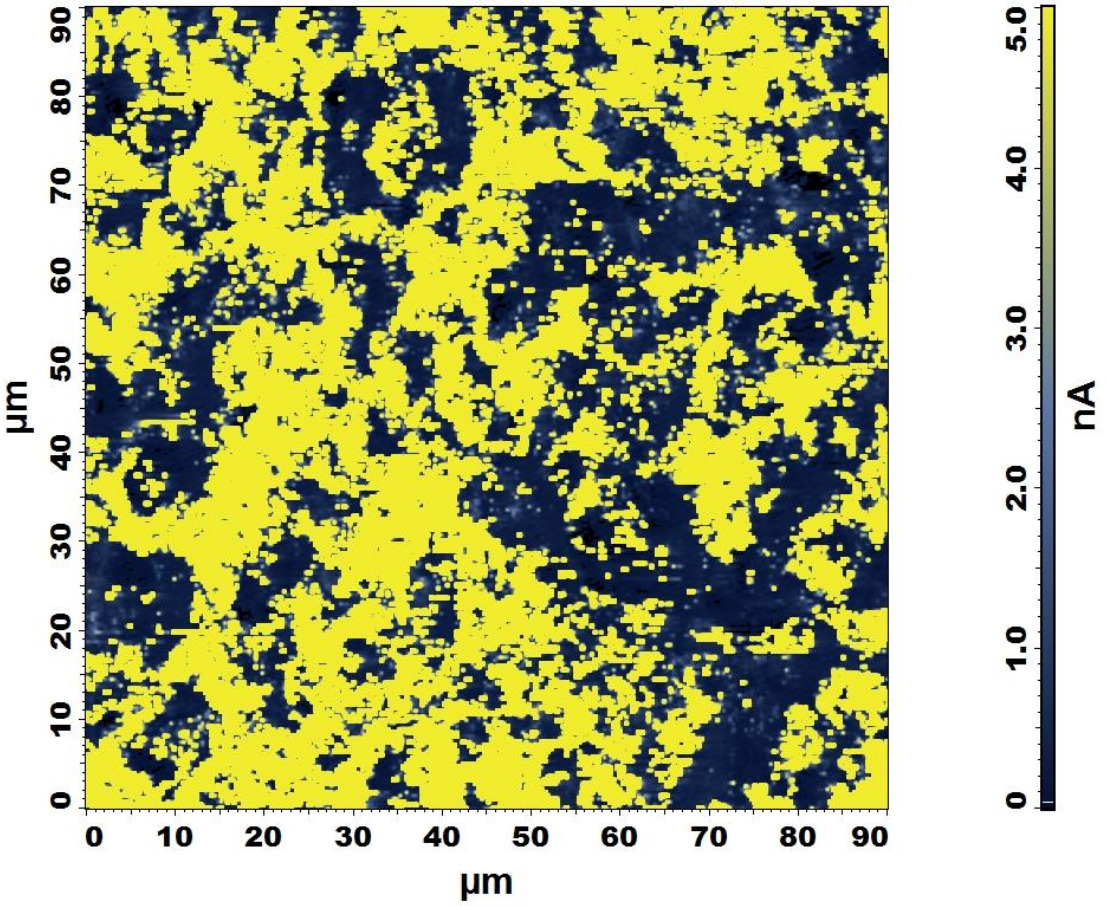

Figure 8b

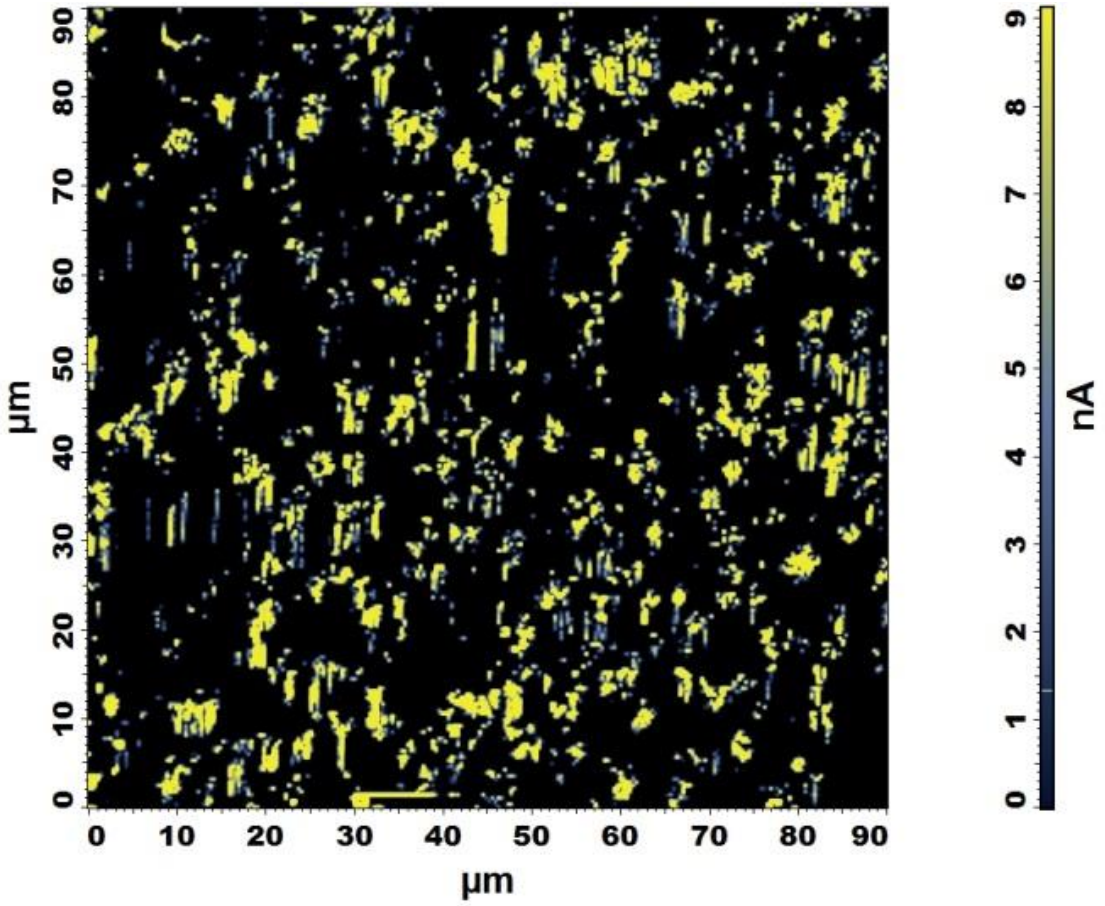

Figure 8c

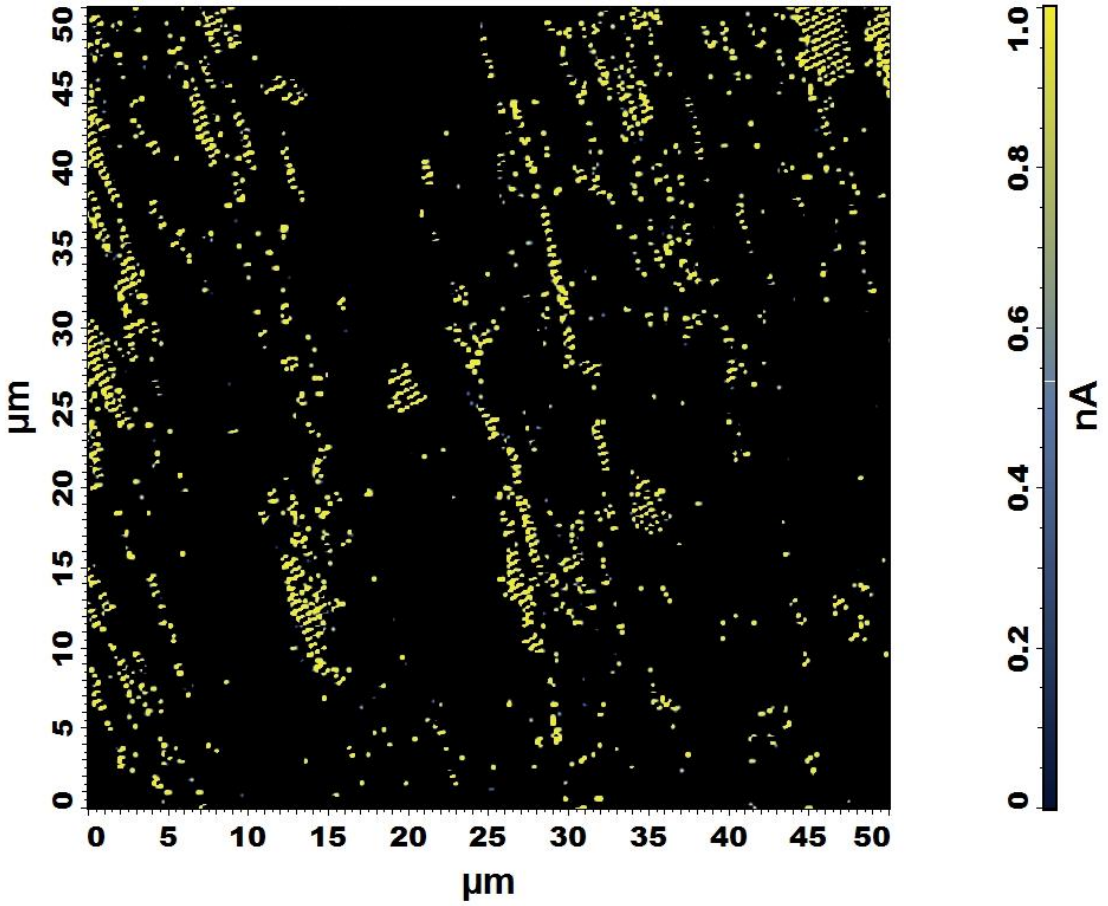

Figure 9

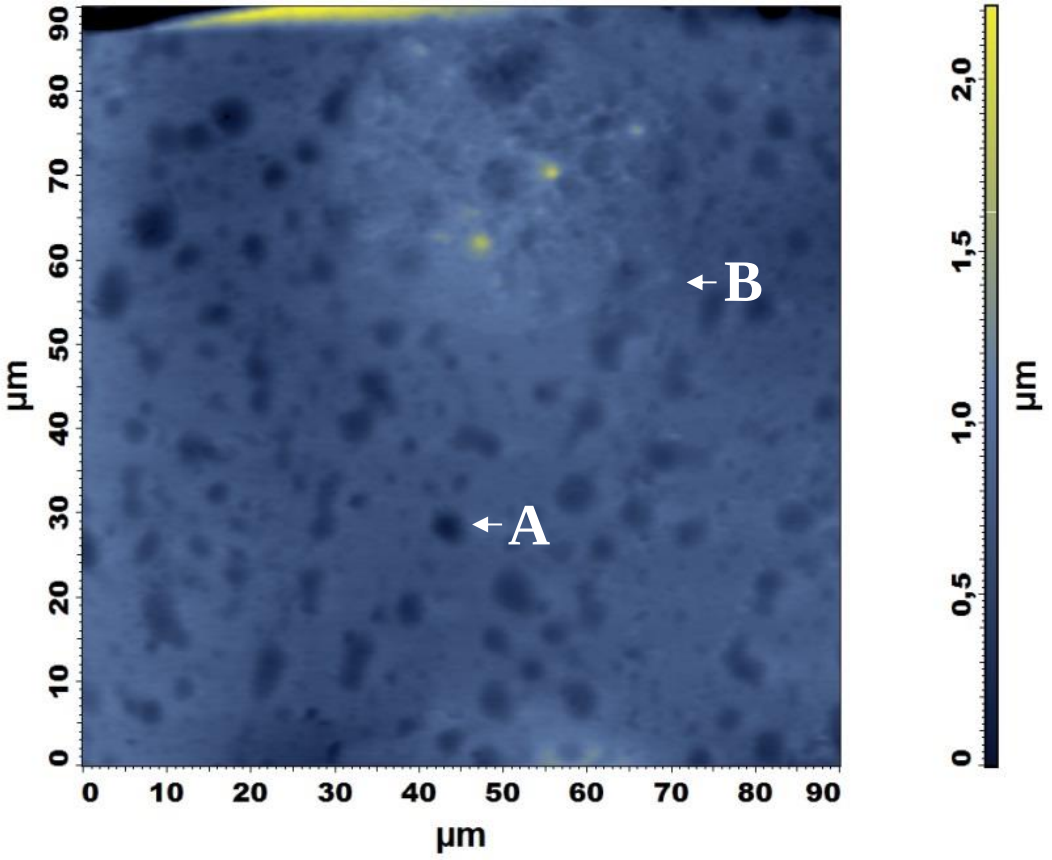

Figure 10

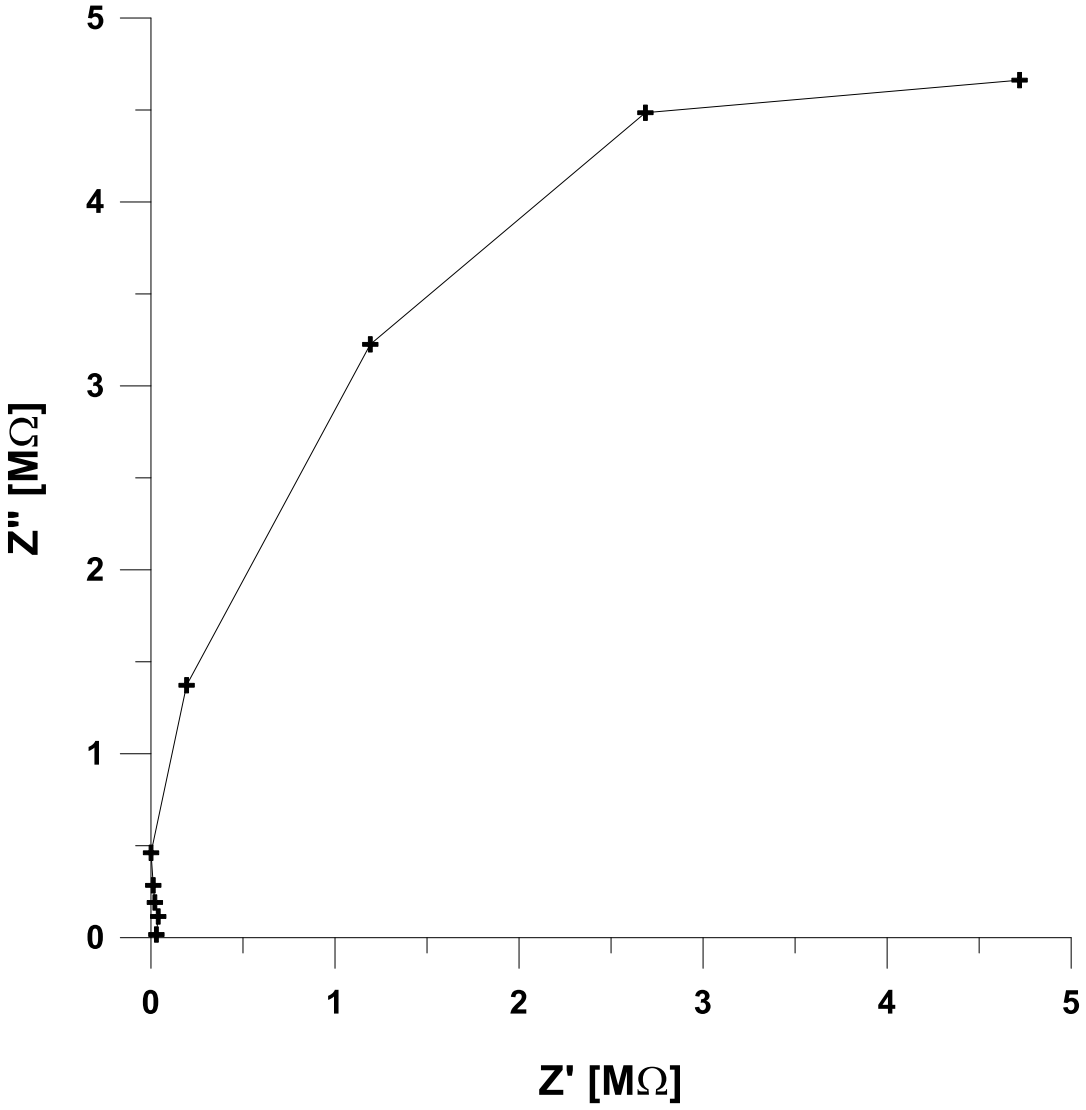

Figure 11

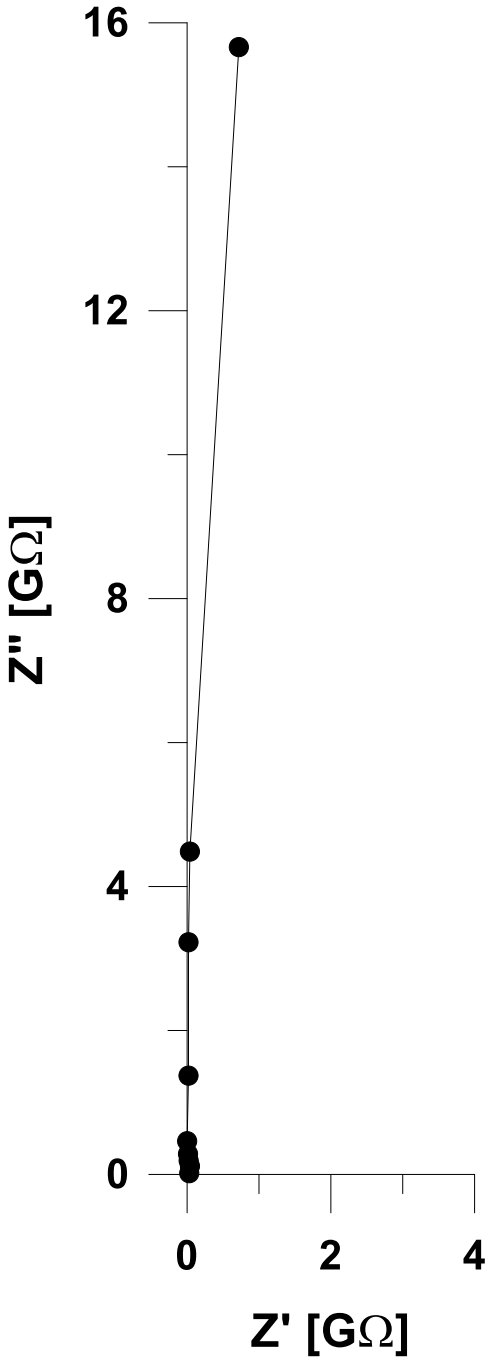

Table 1

Table 1. A comparison of surface roughness (obtained from the AFM measurements) of the investigated types of coatings in as-received state.			
surface roughness parameter	**pure sodium caseinate film**	**propolis-admixed sodium caseinate film**	**propolis-admixed and heated sodium caseinate film**
ten point height S_{10z}	**1.72 µm**	**1.49 µm**	**0.65 µm**